Available Online

JOURNAL OF SCIENTIFIC RESEARCH

J. Sci. Res. **18** (2), 277-293 (2026)

www.banglajol.info/index.php/JSR

Panoramic Behavior of Renyi Holographic Dark Energy in $f(R,T)$ Gravity

K. S. Wankhade[1,*], A. Y. Shaikh[2], A. F. Gotarkar[3]

[1]P.G. Department of Mathematics, Yashwantrao Chavan Science Mahavidyalaya, Mangrulpir-444403. India

[2]Department of Mathematics, Indira Gandhi Mahavidyalaya, Ralegaon-445402, India

[3]Department of Mathematics, Vidnyan Mahavidyalaya, Malkapur-443101, India

Received 28 October 2025, accepted in final revised form 15 February 2026

Abstract

The main motive of this study is to investigate behaviors of Renyi holographic dark energy (RHDE) for anisotropic and homogenous space-time in the framework of $f(R,T)$ gravity. The field equations are solved using (i) the shear scalar of the metric is proportional to the expansion scalar which results a relationship between metric potentials and (ii) special law of variation of Hubble's parameter (Berman (1983)) that yields constant deceleration parameter. The cosmological parameters like energy density, EoS parameter, statefinder parameters, jerk parameter of the model are obtained and discussed their physical significance in the light of the recent scenario of accelerated expansion of the universe and cosmological observations.

Keywords: LRS Bianchi I; RHDE; Modified gravity.

doi: https://dx.doi.org/10.3329/jsr.v18i2.85211 J. Sci. Res. **18** (2), 277-293 (2026)

1. Introduction

The study of outlying Type Ia supernovae revealed the Universe's rapid expansion [1,2], which led to a change in modern cosmology and the appearance of dark energy (DE). The standard ΛCDM model is the result of the usual attribution of a cosmological constant to late-time acceleration in General Relativity (GR). Despite its apparent success, ΛCDM has problems with cosmic coincidence and fine-tuning [3,4], which prompts research into alternate models that use exotic fluids or modify gravitational theory. The $f(R)$ theory of gravitation was initially discussed and established by Buchdahl [5]. Many scholars have studied gravity in various cosmological contexts [6,7] for a survey. $f(R,T)$ gravity was introduced as an extension in which the gravitational Lagrangian is dependent on the trace (T) of the matter energy–momentum tensor as well as the Ricci scalar (R). In their development of field equations inside the metric formalism, Harko *et al*. [8] emphasized that the T-dependence typically results in a nonminimal matter–geometry relationship and non-conserved energy–momentum. These characteristics prompted research on the effects of particle production, dark energy's efficient behavior, and cosmic applications, all of

* *Corresponding author*: wankhade.kishor@rediffmail.com

which directly affected $f(R)$gravity [6,9-11]. A link between matter and geometry results from the obvious dependence on (T), altering the field equations and preventing the conservation of the energy-momentum tensor. This coupling may indicate particle creation, quantum processes, or matter-curvature interactions [8,12]. Regardless of dark energy ideas, this concept offers a unique explanation for the current acceleration of the Universe. A promising area of $f(R,T)$ gravity has seen a lot of research in recent decades, with many functional forms being thoroughly examined to explain late-time acceleration [13-18]. $f(R,T)$ gravity is still a key mechanism for integrating matter and geometry in cosmological dynamics, despite the fact that certain models cast doubt on its cosmic feasibility [19,20].

These advancements coincided with the emergence of holographic dark energy (HDE), a model based on the holographic notion and inspired by quantum gravity. The entropy of a system is proportional to its boundary area rather than its volume, according to this theory [21,22]. To replicate the observed acceleration, a variety of HDE models are tested [23–28]. Entropy-corrected HDE models that are inspired by more general thermodynamic frameworks have been the subject of recent studies. Different entropy generalizations have been used to construct and demonstrate various cosmological models. The Rényi Holographic Dark Energy (RHDE) model [30] can be constructed on the basis of Rényi entropy, which is a non-extensive generalization of Bekenstein-Hawking entropy [29]. RHDE has been the subject of recent studies in a number of cosmological scenarios [31-39], showing increased stability in a non-interacting Universe.

By combining the effects of matter–geometry coupling with non-extensive entropy adjustments, the interaction between $f(R,T)$ gravity and RHDE creates a fresh framework for comprehending the speeding cosmos. This junction has been studied recently. In the context of $f(R,T)$ gravity, Singh *et al.* [40] studied RHDE in anisotropic Bianchi type-I cosmology, obtaining analytical solutions and showing that the model shows a smooth transition from decelerated to accelerated expansion, in agreement with current data. The stability criteria and thermodynamic consistency of non-extensive holographic models with altered $f(R,T)$ gravity backgrounds are examined [41,42]. As Bekova *et al*. [43] showed for Barrow HDE, reconstruction techniques have been applied to determine the functional form of that corresponds to a certain HDE model, suggesting a similar approach appropriate for RHDE frameworks. Based on these findings, it may be possible to overcome the limitations of ΛCDM [44] by incorporating entropy-corrected holographic energy densities into gravitational frameworks to create complex cosmic dynamics. Here, we examine the RHDE model's gravity-related cosmic dynamics, concentrating on the implications for late-time acceleration and cosmological parameter change. This is how the paper is formatted. In Sec. 2, we study the RHDE model, space-time, and field equations, including pressureless dark matter. See Sec. 3 for the calculation of the metric potentials. The main cosmographic tests used to assess the physical plausibility of the model are reviewed in Sec. 4, and the work is concluded in Sec. 5.

2. Metric and Field Equations

Harko *et al.* [8] suggested a modified theory called $f(R,T)$ gravity theory, in which the gravitational matter Lagrangian L_m is determined by an arbitrary function of the Ricci scalar R and the trace of the stress-energy tensor T. The action for this gravity is

$$S = \frac{1}{2k}\int f(R,T)\sqrt{-g}d^4x + \int L_m\sqrt{-g}d^4x \tag{1}$$

where L_m is the matter Lagrangian. The stress energy tensor of matter is defined as

$$T_{ij} = \frac{-2}{\sqrt{-g}}\frac{\partial(L_m\sqrt{-g})}{\partial g^{ij}}\,. \tag{2}$$

Therefore, we obtained $T_{ij} = g_{ij}L_m - \frac{2L_m}{g^{ij}}\,.$ (3)

Varying the action $S$with regard to the metric tensor $g_{\mu\nu}$ yields the gravitational field equations for $f(R,T)$ gravity as

$$f_R(R,T)R_{\mu\nu} = \frac{1}{2}f(R,T)g_{\mu\nu} + f_R(R,T)(g_{\mu\nu}\nabla^\mu\nabla_\mu - \nabla_\nu\nabla_\nu)$$

$$f_R(R,T)R_{\mu\nu} = kT_{\mu\nu} - f_T(R,T)T_{\mu\nu} - f_T(R,T)\theta_{\mu\nu}\,. \tag{4}$$

where, $\theta_{\mu\nu} = g^{\alpha\beta}\frac{\partial T_{\alpha\beta}}{\partial g_{\mu\nu}}, f_R = \frac{\partial f(R,T)}{\partial R}, f_T = \frac{\partial f(R,T)}{\partial T}$, $T_{\mu\nu}$ is the energy momentum tensor, ∇_μ is covariant derivative and $k = \frac{8\pi G}{C^4}$, where $G$and $C$are the Newtonian Gravitational constant and speed of light in vacuum respectively. Three distinct cosmological models of $f(R,T)$ gravity are given by Harko *et al*. [8] viz.

$$f(R,T) = \begin{cases} R + 2f(T) \\ f_1(R) + f_2(T) \\ f_1(R) + f_2(R)f_3(T) \end{cases} \tag{5}$$

Let us consider the functional as $f(R,T) = R + 2f(T)$, where $f(T)$ is any arbitrary function of the trace of the energy-momentum tensor. The resulting field equations are

$$R_{\mu\nu} - \frac{1}{2}Rg_{\mu\nu} = T_{\mu\nu} + 2f'(T)T_{\mu\nu} + [2pf'(T) + f(T)]g_{\mu\nu}. \tag{6}$$

where, overhead prime indicates the differentiation with respect to the argument with particular choice of the function [8] as $f(T) = \mu T$, (7)
where, μ is the constant.

The universe appears to be the same everywhere and in every direction at very large scales. However, the isotropy of the pre-recombination era is not supported by any empirical evidence. Given the known local anisotropies in clusters, superclusters, and galaxies, anisotropic models were studied [45]. We analyse the locally rotationally symmetric (LRS) Bianchi type-I line element, which has been studied by several scholars, in order to clarify and describe the large-scale dynamics of the cosmos in $f(R,T)$ gravity [46-50], as given by

$$ds^2 = dt^2 - A^2(t)dx^2 - B^2(t)(dy^2 + dz^2), \tag{8}$$

where, $A(t)$ and $B(t)$ are the functions of t only. The energy-momentum tensor for DE fluid $\left(T_{\mu\nu}^{(de)}\right)$ and pressure less matter $T_{\mu\nu}^{m}$ are given by

$$T_{\mu\nu}^{(de)} = (\rho_{de} + p_{de})u^{\mu}u_{\nu} - p_{de}g_{\mu\nu};\ T_{\mu\nu}^{(m)} = \rho_m u_{\mu}u_{\nu}. \quad (9)$$

where, ρ_{de} is the DF density, p_{de} is DF pressure, ρ_m the energy density of matter and $u^{\mu}u_{\nu} = 1$, $u^{\mu}u_{\nu} = 0$. The Eos parameter refer to the relation between pressure and energy fluid by

$$\omega_{de} = \frac{p_{de}}{\rho_{de}}. \quad (10)$$

After parametrize the energy-momentum tensor of DE $T_{\mu\nu}^{(de)}$, it can be expressed as

$$T_{\mu\nu}^{(de)} = diag[-p_{de}, -p_{de}, -p_{de}, \rho_{de}]$$
$$T_{\mu\nu}^{(de)} = diag[-\omega_{de}, -\omega_{de}, -\omega_{de}, 1]\rho_{de}. \quad (11)$$

In co-moving system of co-ordinate from equation (11), one finds

$$T_1^1 = T_2^2 = T_3^3 = -\omega_{de}\rho_{de}\ ; T_4^4 = (\rho_m + \rho_{de}). \quad (12)$$

Considering co-moving co-ordinate system, the field equation (6) for the metric (8) with the help of equation (11) can be written as

$$\frac{\dot{B}^2}{B^2} + 2\frac{\ddot{B}}{B} = \omega_{de}\rho_{de} - [\rho_{de} + \rho_m - 3\omega_{de}\rho_{de}]\mu \quad (13)$$

$$\frac{\dot{A}}{A} + \frac{\ddot{B}}{B} + \frac{\dot{A}\dot{B}}{AB} = \omega_{de}\rho_{de} - [\rho_{de} + \rho_m - 3\omega_{de}\rho_{de}]\mu \quad (14)$$

$$\frac{\dot{B}^2}{B^2} + 2\frac{\dot{A}\dot{B}}{AB} = -(\rho_m + \rho_{de}) - [3\rho_m + 3\rho_{de} - \omega_{de}\rho_{de}]\mu \quad (15)$$

where, $(\cdot)$ represent differentiation with respect to time *t*.

The average scale factor $a(t)$ and the spatial volume V are defined by

$$V = a^3 = AB^2. \quad (16)$$

The general form of average Hubble parameter H is defined as

$$H = \frac{\dot{a}}{a} = \frac{1}{3}(H_1 + 2H_2) \quad . \quad (17)$$

Here, $H_1 = \frac{\dot{A}}{A}$ and $H_2 = H_3 = \frac{\dot{B}}{B}$ are directional Hubble parameter along x, y and z axes respectively. The continuity equations can be obtained as

$$\dot{\rho}_m + \dot{\rho}_{de} + 3H(\rho_m + \rho_{de} + p_{de}) = 0. \quad (18)$$

The continuity equations of the matter and DE are respectively obtained as

$$\dot{\rho}_m + 3H\rho_m = 0, \quad (19)$$

and

$$\dot{\rho}_{de} + 3H(\rho_{de} + p_{de}) = 0. \quad (20)$$

Applying the relation $p_{de} = \omega_{de}\rho_{de}$ the barotropic equation of state, the Eos of DE parameter can be

$$\omega_{de} = -1 - \frac{\dot{\rho}_{de}}{3H\rho_{de}}. \quad (21)$$

Using equations (13) and (14), we get

$$-\frac{\dot{B}^2}{B^2} - \frac{\ddot{B}}{B} + \frac{\ddot{A}}{A} + \frac{\dot{A}\dot{B}}{AB} = 0. \quad (22)$$

After solving above equation, we obtain as

$$\frac{A}{B} = C' exp\left(\int \frac{C_0}{V}\, dt\right), \quad (23)$$

where, C' and C_0 are the constants. The expansion scalar θ and shear scalar σ^2 are defined as

$$\theta = \frac{\dot{A}}{A} + \frac{2\dot{B}}{B}. \quad (24)$$

$$\sigma^2 = \frac{1}{3}\left(\frac{\dot{A}}{A} - \frac{\dot{B}}{B}\right)^2. \quad (25)$$

It is observed that the expansion scalar θ is proportional to the shear scalar σ^2 which leads the following relation between A and B as $A = B^n$. (26)

From equation (23) and (26), we get $A = C_1\, exp\left(\frac{nC_0}{(n-1)}\int\frac{1}{V}dt\right)$. (27)

$$B = C_2\, exp\left(\frac{C_0}{(n-1)}\int\frac{1}{V}dt\right). \quad (28)$$

3. Solutions of Field Equations

Equations (13)-(15) are highly non-linear equations with five unknowns such as A, B, w_{de}, ρ_{de}, and ρ_m. It is noteworthy to adopt additional assumptions to solve the field equations. In order to solve $f(R,T)$ field equations, we use the following assumption that Hubble parameter is proportional to volume [51]. According to the law variation of the mean Hubble parameter for LRS Bianchi Type-I metric, we have $H = k(AB^2)^{-m/3}$. (29)
where $k > 0$ and $m \geq 0$are constants. Cosmological models are frequently grouped according to the way the "deceleration parameter" and "Hubble parameter" change over time. During cosmic evolution, these values may show sign shifts, signifying changes between different phases of the cosmos. Tracing this time behavior and identifying the causes underlying it is a primary objective of cosmology. The "deceleration parameter" maintains a constant value of -1 in situations where the "Hubble parameter" remains constant, which is typical of models like "de Sitter and steady-state universes." Such models are usually categorized according to whether they depict expanding or contracting cosmic behaviors, accelerating or decelerating. A rapid expansion model of the cosmos is strongly supported by current observational data. The deceleration parameter of the universe defined by

$$q = -\frac{a\ddot{a}}{\dot{a}^2}. \quad (30)$$

From equations (16), (17) and (29), we get

$$V = AB^2 = D_1 e^{3kt} \text{ for } m = 0, \quad (31)$$

and $V = AB^2 = (mkt + D_2)^{3/m}$ for $m \neq 0$, (32)
where D_1 and D_2 are constants of integration.

3.1. *Exact solutions of RHDE in* $f(R,T)$ *when* $\mathbf{m = 0}$.

Using equations (27), (28) and (30), we obtain

$$A = C_1\, exp\left(\frac{nC_0(e^{-3kt} - 3kD_1')}{-3kD_1(n-1)}\right), \quad (33)$$

and $B = C_2\, exp\left(\frac{C_0(e^{-3kt} - 3kD_1'')}{-3kD_1(n-1)}\right)$. (34)

where D_1' and D_1'' are constants of integration.
The directional Hubble's parameter in the x, x and x axes are given as

$$H_x = \frac{nC_0 e^{-3kt}}{D_1(n-1)}, \quad (35)$$

and $H_y = H_z = \frac{C_0 e^{-3kt}}{D_1(n-1)}$. (36)

The mean Hubble's parameter can be described as $H = \frac{C_0 e^{-3kt}(n+2)}{3D_1(n-1)}$. (37)

The mean anisotropic parameter is given by $\Delta = \frac{2(n-1)^2}{(n+2)^2}$. (38)

Equations (33) and (34) indicate that the average scale factor is non-singular, as an exponential function cannot equal zero. Additionally, the metric potentials A and B are non-zero. It is observed that the scale factors are constant at the starting epoch ($t \to 0$), suggesting that there is no singularity in the model. As cosmic time increases, the scale factors begin to rise and eventually diverge to ∞ when ($t \to \infty$). Therefore, in this instance, the universe's volume is an exponential function that grows from a constant to infinitely enormous over time [52-55]. Moreover, it is noted that when $n = 1$, the mean anisotropy parameter Δ equals zero, indicating the isotropic nature of the Universe. The expansion scalar θ is obtained as

$$\theta = \frac{C_0 e^{-3kt}(n+2)}{D_1(n-1)}. \quad (39)$$

The shear scalar σ^2 is obtained as

$$\sigma^2 = \frac{2{C_0}^2 e^{-6kt}}{3{D_1}^2}. \quad (40)$$

Whether or not the model inflates was indicated by the sign of q. While the negative sign of q denotes inflation, the positive value of q corresponds to the "standard" decelerating model. Interestingly, while the current SNeIa and CMBR measurements favor accelerating models ($q < 0$), both do not completely rule out the decelerating models that are also consistent with these findings. The deceleration parameter is obtained as

$$q = -1 + \frac{9kD_1(n-1)}{C_0(n+2)e^{-3kt}}. \quad (41)$$

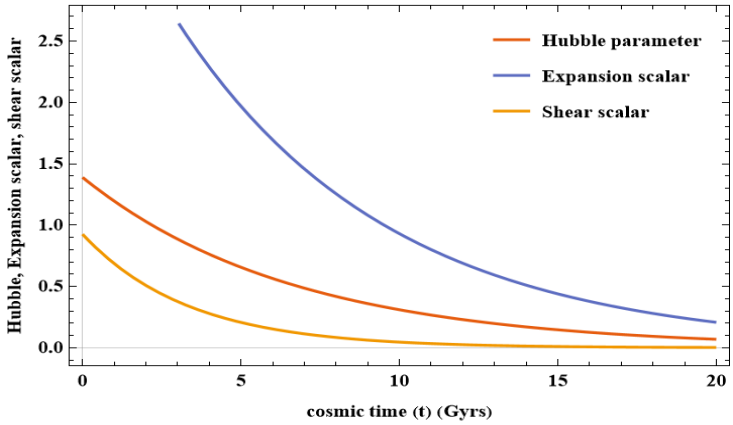

Fig. 1. Hubble parameter, Expansion and shear scalars versus cosmic time.

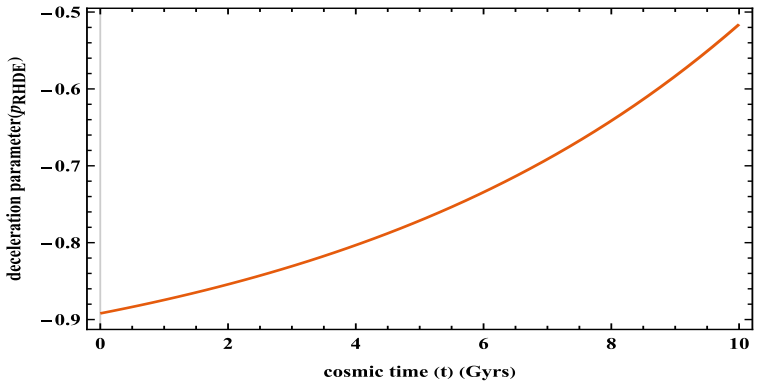

Fig. 2. Deceleration parameter q versus cosmic time t.

Fig. 1 displays the graphical authentication of the Shear Scalar, Expansion Scalar, and Hubble parameter. The Hubble parameter, the expansion scalar, and the shear scalar are high at the beginning of expansion and decrease as the cosmos expands. The constant value of the expansion scalar as both values get closer to zero across long stretches of cosmic time indicates the constancy of the exponential growth. The accelerating model is shown by the deceleration parameter's negative value in Fig. 2. Furthermore, its value falls within a range $-1 \leq q < 0$ that is comparable to the observational data that is currently available. The universe is expanding faster, as indicated by the deceleration parameter $q = -1$, which is consistent with recent SNeIa and CMB findings.

4. Renyi Holographic Dark Energy Model (RHDE)

Let us consider a system with p discrete stats having probability P_i which satisfies the condition $\sum_{I=1}^{p} P_i = 1$, Renyi entropy [56] is a recognized generalized entropy defined as

$$S = \frac{1}{\delta} log \sum_i^p P_i^{1-\delta} \text{and } S_T = \frac{1}{\delta}\sum_{i=1}^{p}\left(P_i^{1-\delta} - P_i\right). \quad (42)$$

where $\delta = 1 - U$ and U is a real parameter, $T = \frac{1}{2\pi L}$, and $L$is the IR cutoff. By using equation (42), we obtain the relation $S = \frac{1}{\delta} log(1 + \delta S_T)$. (43)

In equation (43), the Bekenstein entropy [29] is given by in the form $S_T = \frac{A_1}{4}$ where $A_1 = 4\pi L^2$. This gives the Renyi entropy of the system as $S = \frac{1}{\delta} log(1 + \pi S L^2)$. (44)

The Rényi entropy modifies the area–entropy relation leading to a modified energy density [57,58]. This approach captures quantum gravitational corrections to horizon thermodynamics [30,59,60] and provides flexibility in describing both early and late-time cosmic dynamics [33,34,61]. Using the assumption $\rho_{de} dv \propto Tds$ [30], we get RHDE density (ρ_{RHDE}) as

$$\rho_{RHDE} = \frac{3d^2}{8\pi L^2}(1 + \pi\delta L^2)^{-1}. \quad (45)$$

The Renyi holographic dark energy is calculated by using the Hubble horizon as a candidate for the IR cutoff. i.e. $L = H^{-1}$, as considered in [37,62] and is found to be

$$\rho_{RHDE} = \frac{3d^2H^4}{H^2+\pi\delta}. \tag{46}$$

Using equation (37) in equation (46), we obtain energy density of RHDE as

$$\rho_{RHDE} = \frac{\frac{3d^2{C_0}^4e^{-12kt(n+2)^4}}{81{D_1}^4(n-1)^4}}{\frac{{C_0}^2e^{-6kt(n+2)^2}}{9{D_1}^2(n-1)^2}+\pi\delta}. \tag{47}$$

Using equations (19) and (31) , the energy density of matter is given by

$$\rho_m = \frac{e^{-3kt}}{D_1}. \tag{48}$$

The energy density distribution is found to be a positive decreasing function of time *t*. When the model first begins to expand, that is, when $t = 0$, its energy density is constant. In contrast, when $t > 0$, the energy density of the model is infinite, and at infinite time ($t \to \infty$), it approaches zero, or $\rho_m \to 0$, therefore at infinite expansion, the model is asymptotically empty.

When describing the many epochs of the universe's accelerated and decelerated expansion, the EoS parameter is essential. A stiff fluid is represented by $\omega = 1$, the radiation-dominated phase is represented by $\omega = 1/3$, and the matter-dominated phase is represented by $\omega = 0$. The cosmological constant ($\omega = -1$), quintessence ($-1 < \omega < -1/3$), or the phantom era ($\omega < -1$) are the three possible states described by the EoS parameter for an accelerating universe ($\omega < -1/3$). Using equations (21), (37) and (47) , the EoS parameter of RHDE is obtained as

$$\omega_{RHDE} = \frac{3D_1^2e^{6kt}(n-1)^2}{C_0^5d^2(n+2)^5}\begin{bmatrix}6C_0^2D_1e^{3kt}k(n-1)(n+2)^2+108\pi\delta D_1^3e^{9kt}k(-1+n)^3\\-9\pi\delta C_0D_1^2e^{6kt}(n-1)^2(n+2)-C_0^3(2+n)^3\end{bmatrix} \tag{49}$$

Applying the relation $p_{de} = \omega_{de}\rho_{de}$and using equations (47) and (49) , the RHDE pressure is

$$p_{RHDE} = -1 + \frac{6D_1e^{3kt}k(n-1)\left(C_0^2(2+n)^2+18\pi\delta D_1^2e^{6kt}(n-1)^2\right)}{C_0^3(2+n)^3+9C_0\pi\delta D_1^2e^{6kt}(-1+n)^2(2+n)} \tag{50}$$

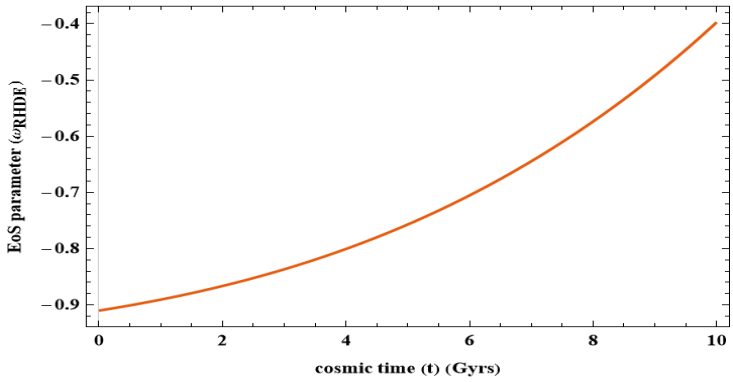

Fig. 3. EoS parameter versus cosmic time *t*.

The evolution of the state parameter equation in the Universe is depicted in Fig. 3. It accurately depicts the speeding universe by remaining within the range of $-1 < \omega_{RHDE} < -\frac{1}{3}$, thus defining the quintessential DE era [63]. We can infer from Fig. 3 that the EoS parameter ω is evolving with a negative value at late times, or right now. The earlier real

matter later on changed to the dark energy dominated era of universe. A divergence-free parameterization and good alignment with empirical constraints are ensured by the smooth shift of ω from $\omega \approx 0$in the matter-dominated era to $\omega < -\frac{1}{3}$ in the quintessence phase, demonstrating how $f(R,T)$ gravity naturally explains cosmic acceleration.

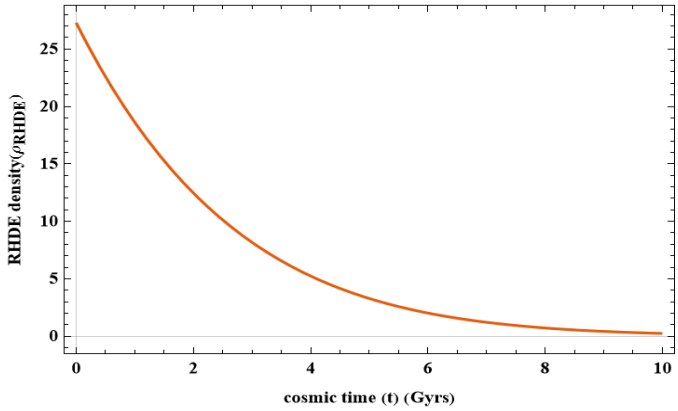

Fig. 4. RHDE energy density versus cosmic time *t*.

The RHDE density remains positive throughout cosmic evolution relative to cosmic time, as seen in Fig. 4, suggesting DE domination in the near future. The energy density (ρ_{RHDE}) graph shows a sharp drop from a high starting value, asymptotically approaching zero as time increases. Fig. 4 makes this pattern very evident, as does the feature of an expanding universe, in which the same quantity of energy is dispersed over a progressively bigger volume, resulting in a diluting effect. This is consistent with the "Big Bang model," which holds that the universe began as a hot, dense state and has since been expanding and contracting. The energy density's smooth and continuous decrease points to a steady, progressive expansion free of sudden shifts.

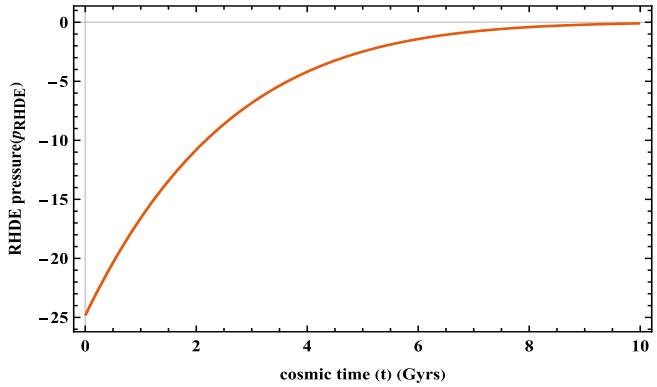

Fig. 5. RHDE pressure versus cosmic time *t*.

The evolution of pressure across cosmic time is depicted in Fig. 5. It suggests that the high level of negative pressure causes the model to accelerate. As it is evident from the host of observational data favoring an accelerated expansion of the universe, it is believed that a negative pressure is required to provide an antigravity effect and to drive the acceleration. The matter density parameter (Ω_m) and RHDE density parameter $(\Omega_{RHDE})$are given respectively by

$$\Omega_m = \frac{\rho_m}{3H^2} = \frac{3e^{3kt}(n-1)^2}{{C_0}^2(n+2)^2}, \tag{55}$$

and $$\Omega_{RHDE} = \frac{\rho_{RHDE}}{3H^2} = \frac{1}{3\left[\frac{{C_0}^2 e^{-6kt}(n+2)^2}{9{D_1}^2(n-1)^2}\right]}\left\{\frac{\frac{3d^2{C_0}^4 e^{-12kt}(n+2)^4}{81{D_1}^4(n-1)^4}}{\frac{{C_0}^2 e^{-6kt}(n+2)^2}{9{D_1}^2(n-1)^2}+\pi\delta}\right\}. \tag{56}$$

One important number in cosmology is the total density parameter Ω, which shows the ratio of the universe's total energy density to its critical energy density. Baryonic matter, or regular matter like atoms and stars, and dark matter are both included in the matter density parameter (Ω_m). It represents the quantity of matter in the cosmos that slows down expansion through gravitational pull, while the dark energy density parameter (Ω_{RHDE}) is linked to the energy that causes the universe to expand more quickly. This is explained by the cosmological constant Λ, which denotes a uniform energy density leaking into space, in the conventional ΛCDM model. The overall density parameter as $\Omega = \Omega_m + \Omega_{RHDE}$, is found to be

$$\Omega = \frac{3e^{3kt}(n-1)^2}{{C_0}^2(n+2)^2} + \frac{1}{3\left[\frac{{C_0}^2 e^{-6kt}(n+2)^2}{9{D_1}^2(n-1)^2}\right]}\left\{\frac{\frac{3d^2{C_0}^4 e^{-12kt}(n+2)^4}{81{D_1}^4(n-1)^4}}{\frac{{C_0}^2 e^{-6kt}(n+2)^2}{9{D_1}^2(n-1)^2}+\pi\delta}\right\}. \tag{57}$$

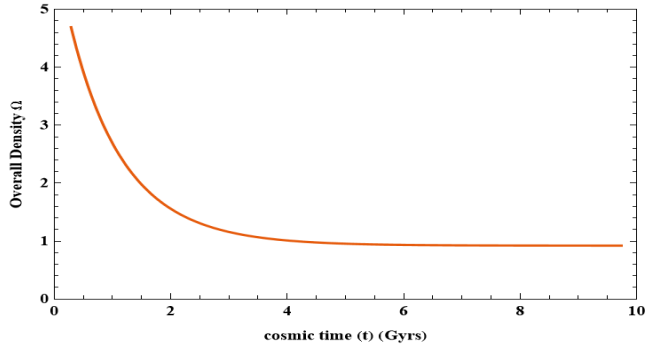

Fig. 6. Overall density versus cosmic time *t*.

The overall density parameter's variation with cosmic time is depicted in Fig. 6. The values of overall density parameter $\Omega > 1, \Omega = 1, \Omega < 1$ corresponds to the open, flat and closed universe respectively. Fig. 6 shows that the value of energy density parameter was large at the early epoch of the universe but approaches to 1 with the passage of time. Thus, the model predicts a flat universe for large times. The present day universe is very close to flat, so the derived model is in accordance with the observations. The general density

parameter decreases during the universe's evolution and, with careful constant selection, converges to 1, suggesting a flat universe consistent with cosmic observations.

5. Jerk Parameter and Statefinder Diagnostics

In cosmology, the jerk parameter is used to identify models that adhere to the ΛCDM framework. The Jerk parameter, $J(t) = q + 2q^2 - \frac{\dot{q}}{H} = \frac{1}{H^3}\frac{\ddot{a}}{a}$, is obtained as

$$J(t) = \left(\frac{9kD_1(n-1)e^{3kt}}{C_0(n+2)} - 1\right) + 2\left(\frac{9kD_1(n-1)e^{3kt}}{C_0(n+2)} - 1\right)^2 - \frac{81k^2{D_1}^2(n-1)^2e^{6kt}}{{e_0}^2(n+2)^2}. \quad (51)$$

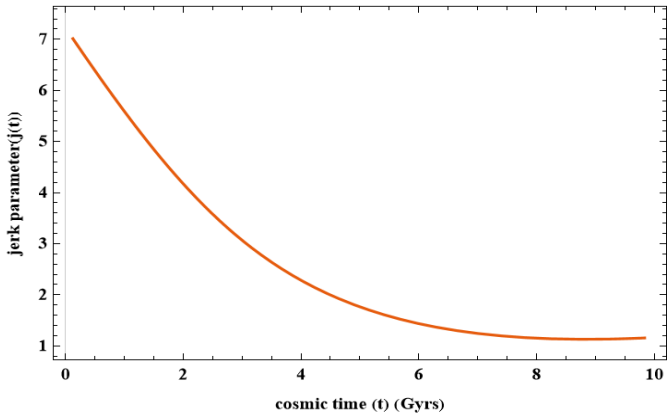

Fig. 7. Approach of jerk parameter against cosmic time.

The statefinder diagnostic, as suggested by Sahni *et al.* [64], is a helpful tool for distinguishing between different cosmological paradigms. The statefinder pair $\{r, s\}$ is given by

$$r = \frac{\ddot{a}}{aH^3} = q + 2q^2 - \frac{\dot{q}}{H};\ s = \frac{r-1}{3\left(q-\frac{1}{2}\right)}, \quad (52)$$

Here, $r = \left(\frac{9kD_1(n-1)e^{3kt}}{C_0(n+2)} - 1\right) + 2\left(\frac{9kD_1(n-1)e^{3kt}}{C_0(n+2)} - 1\right)^2 - \frac{81k^2{D_1}^2(n-1)^2e^{6kt}}{{C_0}^2(n+2)^2}$ (53)

$$s = \frac{\left\{\left(\frac{9kD_1(n-1)e^{3kt}}{C_0(n+2)}-1\right)+2\left(\frac{9kD_1(n-1)e^{3kt}}{C_0(n+2)}-1\right)^2-\frac{81k^2{D_1}^2(n-1)^2e^{6kt}}{{C_0}^2(n+2)^2}\right\}-1}{3\left(\frac{9kD_1(n-1)e^{3kt}}{C_0(n+2)}-\frac{3}{2}\right)}. \quad (54)$$

Fig. 7 shows the approach of the jerk parameter with advancement in cosmic time. The ΛCDM framework is revealed when it tends to approach 1 at late times after beginning with positive values in the early era. As it crosses the point $(r, s) = (1,0)$, the visualization of $r$against$s$ is shown in Fig. 8 and tends to approach the ΛCDM model in the near future, which is similar to the results presented in [65-70].

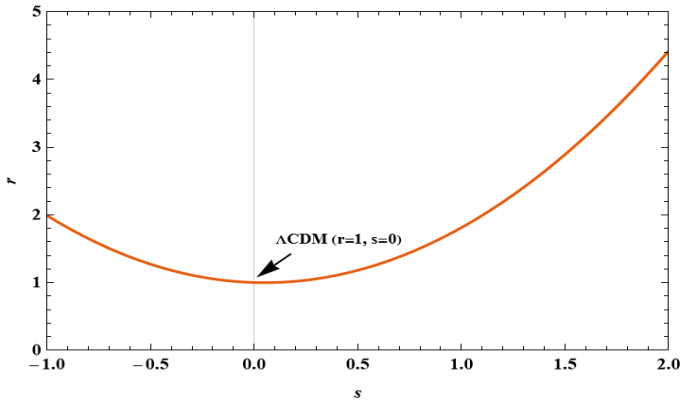

Fig. 8. Approach of *r* against *s*.

6. Observational Data and Methodology

The several observational datasets can now be used to restrict the parameters(H_0, k). We apply the conventional Bayesian technique to accomplish an inspection of the observational data, alongside we use the MCMC methodology for ascertaining the posterior allocations of parameters . Furthermore, MCMC analysis is conducted exploiting the emcee structure.To finish the analysis in this work, we employed the Hubble measurements, often known as the Hubble data. The optimal parameter fits are determined through the application of the subsequent likelihood function $\mathcal{L} \propto exp\left(\frac{-\chi^2}{2}\right)$, where the pseudo chi-squared function is denoted by χ^2. We start by evaluating the parameter space priors, which are $(50.0 < H_0 < 100.0)$ to account for every potential Hubble parameter scenario and $-0.5 < k < 0.5$ to obtain every scenario of the Universe's expansion. Remember that our cosmological model must also fit the observable datasets. The following section discusses the χ^2functions for different datasets. Cosmologists frequently use a statistical tool called the chi-square (χ^2) test to determine the degree of agreement between the theoretical predictions and observable $H(z)$ measurements. A statistic that measures how well the model and the data fit each other is computed using the χ^2 test. A closer fit between the model and observations is shown by smaller χ^2 values.

6.1. *Hubble datasets*

The model's parameter along with the most recent value of the Hubble parameter H_0 are then determined by considering 31 Hubble data sets within the redshift interval $(0.07 < z < 1.965)$. To find the mean value of the parameters k and H_0, the corresponding chi-square function is expressed as

$$\chi^2(H_0, k) = \sum_{i=0}^{31} \frac{[H_{th}(i) - H_{ob}(i)]^2}{\sigma(i)^2}, \tag{55}$$

with $H_{th}(i)$ and $H_{ob}(i)$ specify the $H(z)$'s theoretical and observed values respectively while $\sigma(i)$'s stands for corresponding errors in $H_{ob}(i)$.

6.2. *Pantheon datasets*

The parameter k and H_0 are derived from analysing 1048 data points associated with the Pantheon Type Ia supernova collection. This dataset includes 1048 estimations of apparent magnitudes, with redshifts ranging from 0.01 to 2.3. In standard cosmology, the distance modulus $\mu(z)$ can be estimated through $\mu = m_B - M = 5\,log(d_l(z)) + 25$. Here, the apparent magnitude is specified by m_B , whereas the absolute magnitude is represented by $M$and where m_B is the apparent magnitude, M is the absolute magnitude and, $E(z) = \frac{H(z)}{H_0}$ being the non-dimensional measure for expansion trend, $d_l(z) = \frac{c(1+z)}{H_0}\int_0^z \frac{dz}{E(z)}$ describes the luminosity distance. It is perceived all supernovae possess a uniform absolute magnitude, we may apply the method to find absolute magnitude *M* using the supernova 2002 cr that display an estimate of m_B= 13.907 ± 0.1982 regarding a tiny redshift of z = 0.0101 and $M = 5\,log_{10}\left(\frac{H_0}{c}\right) - 1.093$.

The following apparent magnitude equation is $m_B = 5\,log_{10}\left(\frac{d_l(z)H_0}{c}\right) + 23.907$.The relevant chi-square function is described as: $\chi^2_{Pan}(H_0, k) = \sum_{i=0}^{1048} \frac{[\mu_{th}(i) - \mu_{ob}(i)]^2}{\sigma(i)^2}$, (56)
Here, μ_{th} and μ_{obs} are theoretical and observational distance modulus while σ_i^2describes variance.

6.3. *BAO datasets*

The 6dFGS, SDSS, and Wiggle Z surveys that make up the Baryonic Acoustic Oscillation (BAO) collection include BAO measurements at the six distinct redshifts listed in Table 1. The sound horizon r_s at the photon decoupling epoch z use the following relation to determine the characteristic scale of BAO.

Table 1 .Values of $\frac{d_A(z_*)}{D_v(z_{BAO})}$ for distinct values of z_{BAO}.

z BAO	0.106	0.2	0.35	0.44	0.6	0.73
$\frac{d_A(z_*)}{D_v(z_{BAO})}$	30.95±1.46	17.55±0.60	10.11±0.37	8.44±0.67	6.69±0.33	5.45±0.31

Now $r_s(z_*) = \frac{c}{\sqrt{3}}\int_0^{\frac{1}{1+z_*}} \frac{da}{a^2 H(a)\sqrt{1+\left(\frac{3\Omega_{0b}}{4\Omega_{0r}}\right)^a}}$. (57)

Here Ω_{ob} and Ω_{or} represent present densities of baryons and photons respectively. Six-point BAO datasets for $\frac{d_A(z_*)}{D_v(z_{BAO})}$are used in this work . In this case, the photon decoupling epoch redshift is calculated as $z_* \approx 1091$ and $D_v(z) = \left(\frac{d_A(z)^2 z}{H(z)}\right)^{\frac{1}{3}}$ is the dilation scale, and $d_A(z) = \int_0^z \frac{dz'}{H(z')}$ is the co-moving angular diameter distance. For the BAO distance datasets, the chi square function is applied as $\chi^2_{BAO} = X^T C^{-1} X$. (58)

6.4. *Observational finding*

By suppressing the composite chi-squared function $\chi^2_H + \chi^2_{Pan} + \chi^2_{BAO}$, limits on the parameters that describe our cosmological model for both perspectives are determined using an assortment of $H(z)$ + Pantheon datasets + BAO datasets.

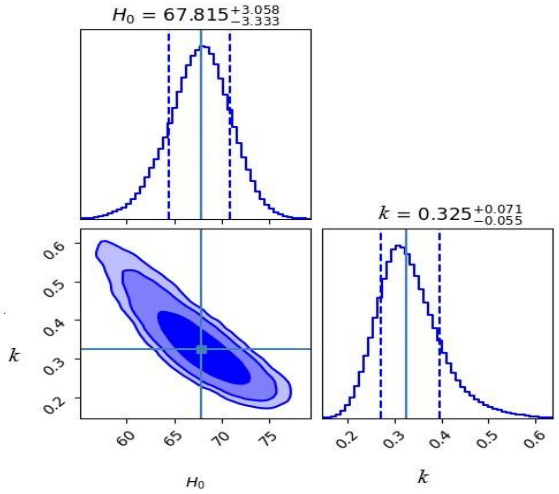

Fig. 9. The likelihood contours at 1−σ and 2−σ over the model parameters through an analysis of the $H(z) +$ and Pantheon datasets+ BAO datasets.

By using the aforementioned combined $H(z) +$ and Pantheon datasets+ BAO datasets, we obtained the best fit values of the model parameter k as shown in Fig. 9 with 1−σ and 2−σ likelihood contours. For $m = 0, D_1 = 1$, the best-fit values obtained are $H_0 = 67.815^{+3.058}_{-3.333}$ and $k = 0.325^{+0.071}_{-0.055}$.

7. Conclusions

The physical plausibility of the model is evaluated in relation to ΛCDM and various other HDE variants through a meticulous examination of essential diagnostics, including the deceleration parameter, the equation of state, and the statefinder parameters. This methodology enhances comprehension of the relationship between non-extensive entropy and the coupling of matter and geometry, while simultaneously providing a route toward a coherent portrayal of cosmic evolution. Our RHDE model analyses the cosmic dynamics of the Universe in $f(R,T)$ gravity, focusing on late-time acceleration and the evolution of cosmological parameters. The model does not have physical singularities. The negative deceleration parameter indicates an accelerating model . The EOS parameter changes over time, indicating the quintessence DE era. The RHDE density remains positive throughout cosmic evolution, indicating DE dominance in the near future. Our model indicates an accelerating cosmos due to negative pressure. The overall density parameter diminishes as

the universe evolves, it converges to 1, indicating a flat universe in alignment with observational data while the approach r against s crosses the ΛCDM limit during the cosmic development. . For $m = 0, D_1 = 1$, the best-fit values obtained are $H_0 = 67.815^{+3.058}_{-3.333}$ and $k = 0.325^{+0.071}_{-0.055}$. It is concluded that, the current framework adeptly elucidates the ongoing cosmic acceleration, with remaining anisotropic effects offering a possible insight into the dynamics of the early universe.

References

1. A. G. Riess, A. V. Filippenko, P. Chalsis, A. Clocchiatti, A. Diercks et al., Astron. J. **116**, 1009 (1998). https://doi.org/10.1086/300499
2. S. Perlmutter, G. Aldering, G. Goldhaber, R. A. Knop, P. Nugent et al., Astrophys. J. **517**, 565 (1999). https://doi.org/10.1086/307221
3. S. Weinberg, Rev. Mod. Phys. **61**, 1 (1989). https://doi.org/10.1103/RevModPhys.61.1
4. P. J. E. Peebles and B. Ratra, Rev. Mod. Phys. **75**, 559 (2003). https://doi.org/10.1103/RevModPhys.75.559
5. H. A. Buchdahl,Mon. Not. R. Astron. Soc. **150**, 1 (1970). https://doi.org/10.1093/mnras/150.1.1
6. A. De Felice and S. Tsujikawa, Living Rev. Relativ. **13**, ID 3 (2010). https://doi.org/10.12942/lrr-2010-3
7. V. Faraoni, General Relativity and Quantum Cosmology (2008). https://doi.org/10.48550/ARXIV.0810.2602
8. T. Harko, F. S. N. Lobo, S. Nojiri, and S. D. Odintsov, Phys. Rev. D **84**, ID 024020 (2011). https://doi.org/10.1103/PhysRevD.84.024020
9. S. Capozziello, P. Martin-Moruno, and C. Rubano, Phys. Lett. B **664**, 12 (2008). https://doi.org/10.1016/j.physletb.2008.04.061
10. S. Capozziello and M. De Laurentis, Ann. Phys. **524**, 545 (2012). https://doi.org/10.1002/andp.201200109
11. S. Nojiri and S. D. Odintsov, High Energy Physics - Theory (2008). https://doi.org/10.48550/arXiv.0807.0685
12. P. H. R. S. Moraes and P. K. Sahoo, Eur. Phys. J. C **77**, 480 (2017). https://doi.org/10.1140/epjc/s10052-017-5062-8
13. K. R. Mule, S. P. Gaikwad, and V. G. Mete, New Astron. **105**, ID 102087 (2024). https://doi.org/10.1016/j.newast.2023.102087
14. P. K. Sahoo, B. Mishra, and S. K. Tripathy, Indian J. Phys. **90**, 485 (2016). https://doi.org/10.1007/s12648-015-0759-8
15. M. J. S. Houndjo, Int. J. Mod. Phys. D **21**, ID 1250003 (2012). https://doi.org/10.1142/S0218271812500034
16. R. Zaregonbadi, M. Farhoudi, and N. Riazi, Phys. Rev. D **94**, ID 084052 (2016). https://doi.org/10.1103/PhysRevD.94.084052
17. S. B. Fisher and E. D. Carlson, Phys. Rev. D **100**, ID 064059 (2019). https://doi.org/10.1103/PhysRevD.100.064059
18. H. Shabani and M. Farhoudi, Phys. Rev. D **88**, ID 044048 (2013). https://doi.org/10.1103/PhysRevD.88.044048
19. E. Barrientos, F. S. N. Lobo, S. Mendoza, G. J. Olmo, and D. Rubiera-Garcia, Phys. Rev. D **97**, ID 104041 (2018). https://doi.org/10.1103/PhysRevD.97.104041
20. H. Velten and T. R. P. Caramês, Phys. Rev. D **95**, ID 123536 (2017). https://doi.org/10.1103/PhysRevD.95.123536
21. G. 'T Hooft (World Scientific, Erice, Sicily, Italy, 2001) pp. 72-100. https://doi.org/10.1142/9789812811585_0005
22. W. Fischler and L. Susskind, High Energy Physics-Theory (1998). https://doi.org/10.48550/arXiv.hep-th/9806039

23. S. Nojiri and S. D. Odintsov, Eur. Phys. J. C **77**, 528 (2017). https://doi.org/10.1140/epjc/s10052-017-5097-x
24. D. Pavón and W. Zimdahl, Phys. Lett. B **628**, 206 (2005). https://doi.org/10.1016/j.physletb.2005.08.134
25. A. Y. Shaikh and A. P. Jenekar, East Eur. J. Phys. **3**, 26 (2025). https://doi.org/10.26565/2312-4334-2025-3-03
26. A. Y. Shaikh, A. P. Jenekar, and S. M. Shingne, East Eur. J. Phys. **3**, 4 (2025). https://doi.org/10.26565/2312-4334-2025-3-01
27. D. D. Pawar, R. V. Mapari, and P. K. Agrawal, J. Astrophys. Astron. **40**, 13 (2019). https://doi.org/10.1007/s12036-019-9582-5
28. A. Pradhan, V.K. Bhardwaj, A. Dixit, and S. Krishnannair, Int. J. Mod. Phys. A **36**, ID 2150256 (2021). https://doi.org/10.1142/s0217751x21502560
29. J. D. Bekenstein, Phys. Rev. D **7**, 2333 (1973). https://doi.org/10.1103/PhysRevD.7.2333
30. H. Moradpour, S. A. Moosavi, I. P. Lobo, J. P. M. Graça, A. Jawad, and I. G. Salako, Eur. Phys. J. C **78**, 829 (2018). https://doi.org/10.1140/epjc/s10052-018-6309-8
31. S. Ghaffari, A. H. Ziaie, V. B. Bezerra, and H. Moradpour, Mod. Phys. Lett. A **35**, ID 1950341 (2020). https://doi.org/10.1142/S0217732319503413
32. U. K. Sharma and V. C. Dubey, New Astron. **80**, ID 101419 (2020). https://doi.org/10.1016/j.newast.2020.101419
33. A. Dixit, V. K. Bhardwaj, and A. Pradhan, Eur. Phys. J. Plus **135**, 831 (2020). https://doi.org/10.1140/epjp/s13360-020-00850-6
34. U. Y. D. Prasanthi and Y. Aditya, Results Phys. **17**, ID 103101 (2020). https://doi.org/10.1016/j.rinp.2020.103101
35. V. C. Dubey, A. K. Mishra, and U. K. Sharma, Astrophys. Space Sci. **365**, ID 129 (2020). https://doi.org/10.1007/s10509-020-03846-x
36. A. Saha, S. Ghose, A. Chanda, B.C. Paul, Ann. Phys. **426**, ID 168403 (2021). https://doi.org/10.1016/j.aop.2021.168403
37. K. S. Wankhade, A. Shaikh, and S. N. Khan, East Eur. J. Phys. **3**, 87 (2023). https://doi.org/10.26565/2312-4334-2023-3-06
38. M. V. Santhi, T. Chinnappalanaidu, and M. Tripathy, Indian J. Phys. **98**, 3393 (2024). https://doi.org/10.1007/s12648-023-03051-w
39. A. Y. Shaikh, Indian J. Phys. **98**, 4623 (2024). https://doi.org/10.1007/s12648-024-03151-1
40. M. S. Singh and S. S. Singh,New Astron. **72**, 36 (2019). https://doi.org/10.1016/j.newast.2019.03.007
41. S. N. Gashti and B. Pourhassan, Eur. Phys. J. C **85**, 435 (2025). https://doi.org/10.1140/epjc/s10052-025-14152-7
42. A. G. Shalaby, V. K. Oikonomou, and G. G. L. Nashed, Symmetry **13**, 75 (2021). https://doi.org/10.3390/sym13010075
43. G. Bekova, A. Altaibayeva, U. Ualikhanova, and S. Chattopadhyay, Eur. Phys. J. C **85**, 1135 (2025). https://doi.org/10.1140/epjc/s10052-025-14843-1
44. N. Shahhoseini, M. Malekjani, and A. Khodam-Mohammadi, Eur. Phys. J. C **85**, 53 (2025). https://doi.org/10.1140/epjc/s10052-025-13781-2
45. D. Saadeh, S. M. Feeney, A. Pontzen, H. V. Peiris, and J. D. McEwen, Phys. Rev. Lett. **117**, ID 131302 (2016). https://doi.org/10.1103/PhysRevLett.117.131302
46. P. K. Sahoo and M. Sivakumar, Astrophys. Space Sci. **357**, 60 (2015). https://doi.org/10.1007/s10509-015-2264-0
47. B. K. Bishi, S. K. J. Pacif, P. K. Sahoo, and G. P. Singh, Int. J. Geom. Methods Mod. Phys. **14**, ID 1750158 (2017). https://doi.org/10.1142/s0219887817501584
48. U. K. Sharma, R. Zia, A. Pradhan, and A. Beesham, Res. Astron. Astrophys. **19**, ID 055 (2019). https://doi.org/10.1088/1674-4527/19/4/55
49. V. Singh and A. Beesham, Astrophys. Space Sci. **365**, 125 (2020). https://doi.org/10.1007/s10509-020-03839-w

50. R. K. Tiwari, D. Sofuoğlu, V. K. Dubey, Int. J. Geom. Methods Mod. Phys. **17**, ID 2050187 (2020). https://doi.org/10.1142/S021988782050187X
51. M.S. Berman, Il Nuovo Cimento B Ser. **74**, 182 (1983). https://doi.org/10.1007/BF02721676
52. Y. F. Cai and X. Zhang, J. Cosmol. Astropart. Phys. **2009**, ID 003 (2009). https://doi.org/10.1088/1475-7516/2009/06/003
53. T. Katsuragawa, S. Nojiri, and S. D. Odintsov, Phys. Rev. D **110**, ID 064014 (2024). https://doi.org/10.1103/PhysRevD.110.064014
54. S. Nojiri, S. D. Odintsov, and S. Tsujikawa, Phys. Rev. D **71**, ID 063004 (2005). https://doi.org/10.1103/PhysRevD.71.063004
55. S. Bahamonde, S. D. Odintsov, V. K. Oikonomou, and M. Wright, Ann. Phys. **373**, 96 (2016). https://doi.org/10.1016/j.aop.2016.06.020
56. J. C. Baez, Entropy **24**, 706 (2022). https://doi.org/10.3390/e24050706
57. W. Hao, Commun. Theor. Phys. **52**, 743 (2009). https://doi.org/10.1088/0253-6102/52/4/35
58. R. G. Cai, L.-M. Cao, and Y.-P. Hu, J. High Energy Phys. **2008**, ID 090 (2008). https://doi.org/10.1088/1126-6708/2008/08/090
59. P. Jizba and T. Arimitsu, Ann. Phys. **312**, 17 (2004). https://doi.org/10.1016/j.aop.2004.01.002
60. H. Moradpour, S. A. Moosavi, I. P. Lobo, J. P. M. Graça, A. Jawad, and I. G. Salako, Eur. Phys. J. C **78**, 829 (2018). https://doi.org/10.1140/epjc/s10052-018-6309-8
61. M. K. Alam, S. S. Singh, and L. A. Devi, Astrophysics **66**, 383 (2023). https://doi.org/10.1007/s10511-023-09798-8
62. S. Srivastava and U. K. Sharma, Int. J. Geom. Methods Mod. Phys. **18**, ID 2150014 (2021). https://doi.org/10.1142/s0219887821500146
63. Y. B. Wu, S. Li, M. H. Fu, and J. He, Gen. Relativ. Gravit. **39**, 653 (2007). https://doi.org/10.1007/s10714-007-0412-8
64. V. Sahni, T. D. Saini, A. A. Starobinsky, and U. Alam, J. Exp. Theor. Phys. Lett. **77**, 201 (2003). https://doi.org/10.1134/1.1574831
65. A.Y. Shaikh, Eur. Phys. J. Plus **138**, 301 (2023). https://doi.org/10.1140/epjp/s13360-023-03931-4
66. A. Y. Shaikh and A. P. Jenekar, Int. J. Geom. Methods Mod. Phys. (2025). https://doi.org/10.1142/S0219887826500222
67. S. P. Gaikwad and K. R. Mule, J. Sci. Res. **16**, 757 (2024). https://dx.doi.org/10.3329/jsr.v16i3.72268
68. S. Samdurkar, R. Pathekar, R. Tambatkar, and S. Bawnerkar, J. Sci. Res. **17**, 367 (2025). https://dx.doi.org/10.3329/jsr.v17i2.74136
69. K. N. Pawar and M. D. Netnaskar, J. Sci. Res. **17**, 407 (2025). https://dx.doi.org/10.3329/jsr.v17i2.75357
70. A. R. Gupta and R. N. S. Sisodiya, J. Sci. Res. **17**, 821 (2025). https://dx.doi.org/10.3329/jsr.v17i3.79078